

# ANALYSIS AND DETECTION OF EEG TRANSIENT WAVES DURING SLEEP

**Ionescu Ana-Maria<sup>1</sup>, Dumitrescu Cătălin<sup>2</sup>, Copaci Carmen<sup>3</sup>, Iliescu Dan<sup>1</sup>, Hangan Tony<sup>1</sup>, Bobe Alexandru<sup>4</sup>**

<sup>1</sup> Faculty of Medicine, “Ovidius” University, Constanța, Romania

<sup>2</sup> Department of Artificial Intelligence, University Politehnica of Buchares, Romania

<sup>3</sup> UTI Grup SA

<sup>4</sup> Faculty of Mathematics and Informatics, “Ovidius” University, Constanța, Romania

**Dan Iliescu**

Faculty of Medicine, Univeristy „Ovidius” of Constanta,  
Universitatii Alee No. 1, Campus B, Constanta, Romania

email: dan@anatomie.ro

phone: +40 722973928

## ABSTRACT

*Electroencephalogram (EEG) analysis consists of locating signal structures in time and frequency. A detection method based on the Matching Pursuit Algorithms finds the suboptimal solution of the function optimal linear expansion over a redundant waveform dictionary. This paper has put forth a method for the automatic detection and analysis of transient waves during sleep based on the matching pursuit method with a real dictionary of Gabor functions. Each wave peak is described in terms of natural parameters. In this context, there have been confirmed several literature hypotheses regarding the spatial, temporal, and frequency distribution of transient waves during sleep, and their relationships with slow wave brain activity. Mastery and expertise in clinical EEG interpretation is one of the most desirable diagnostic clinical skills in interpreting seizures, epilepsy, sleep disorder, biomarkers for early diagnosis of Parkinson's and Alzheimer's disease, and other neurocognitive studies.*

*Keywords: matching pursuit, discrete Gabor functions, EEG analysis, non-stationary signals, multicomponent signals*

## Introduction

The first success in automatic EEG analysis was the introduction of the Fast Fourier Transform in 1965 which is a development of the Fourier Transform (FT). The Fourier transform fulfills the prediction criterion and performs a category of information - the spectral distribution of the signal energy. Nevertheless, FT can lead to statistical errors and is severely influenced by the assumption that the signal is either infinite or periodically outside the measurement window. However, until now, FFT has remained the main method of signal processing used for biomedical signal analysis. Parametric methods, such as the

autoregressive model, do not have the “window” effect and yield estimates with better statistical properties because they no longer assume the signal to be outside the measurement window. However, as in the case of FT, the signal must be stationary. Spectral methods, such as the Fourier transform and autoregressive models, have some natural limitations. They provide global features of the entire segment under analysis while the signal structures that last shorter than the measurement window cannot be identified. According to state-of-the-art expertise, the information processed by the brain is encoded by the dynamic changes of electrical activity in time, frequency and space. A complete

description of these phenomena would require a very good time-frequency resolution that cannot be obtained with the FFT or autoregressive model. Indeed, there are plenty of cases where the global characteristics of the entire analyzed segment are needed. Furthermore, in some cases, time-frequency analyses cannot provide the type of information given by the multi-channel autoregressive model, e.g., the direction of information flow between electrodes. Since none of the approximations presented satisfies all the requirements, we shall introduce a new method in the processing of biomedical signals - the Gabor adaptive representation for real functions.

This project addresses the problem of detecting sleep spindles and K-complexes in human sleep EEG as a biological marker for memory consolidation. Sleep spindles and K-complexes aid in classifying stage 2 NREM human sleep. Both of them play a critical role in system consolidation of long term declarative and procedural memories, having a significant impact on human performance.

Neurological and psychiatric conditions like Alzheimer's disease (AD) and schizophrenia are associated with decreased memory performance and reduced spindle activity during sleep. Similarly, a decline in learning capabilities in the elderly correlates with diminished sleep spindle activity in prefrontal cortical areas. These examples complement the studies in healthy subjects by demonstrating a relationship between spindles and memory also under conditions of decreased performance.

### **The Matching Pursuit adaptive representation**

The natural limitations of the classical transform with damped waves in biomedical signal processing are due to the relatively small set of waveforms used to express signal dispersion. It may be said that the dictionary used in wavelet transformation is limited. In the case of the orthogonal transform with package damped wavelets, one must work with the smallest possible dictionary - on an orthonormal basis.

A natural language is redundant: many

words are very close in meaning. Because of this factor, we can express very subtle and complicated ideas in relatively few words. On the other hand, let us suppose that the same ideas (feelings, thoughts) are described by a person using a limited dictionary. Not only will the expressions increase in size, but it will lose much of significance and, of course, elegance.

Dictionaries with low redundancy (or without, as in the case of a base) are convenient for both calculations and interpretation. However, if the main purpose is to adapt the representation, the "dictionary" of the basic functions should be increased. A large and redundant basic waveform dictionary can be generated, for example, by scaling, translation and, unlike the wavelet transform, by the modulation of a single window function  $g(t)$ :

$$g_I(t) = \frac{1}{\sqrt{s}} g\left(\frac{t-u}{s}\right) e^{ix} \quad [1]$$

where  $s > 0$  - is the scale este scala,  
 $x$  - modulation frequency,  
 $u$  - translation.

Index  $I = (s, x, u)$  describes the set of parameters. The window function  $g(t)$  is usually even and its energy is mostly concentrated around  $u$  within a time frame proportional to  $s$ . In the frequency domain the energy is mostly concentrated around  $x$  with a scattering proportional to  $1/s$ . The minimum time-frequency dispersion is obtained if  $g(t)$  is Gaussian.

The dictionaries of the windowed Fourier transform and of the damped waves transform may be obtained as subsets of this dictionary defined by some restrictions in the choice of parameters. In the case of the Fourier transform window, scale  $s$  is constant - equal to the window wavelength - and parameters  $u$  and  $x$  are uniformly sampled. In the case of the wavelet transform, the frequency modulation is limited by the frequency parameter restriction  $x = x_0/s, x_0 = \text{const}$ .

One is left to choose from such a dictionary waveform that best fit the signal structures, that is, to best express the signal dispersion

An optimal approximation  $e$  may be defined as an extension that minimizes the approximation error  $e$  of signal  $f$  by  $M$  waveforms:

$$\varepsilon = |f - \sum (f, g_I) g_I| - \min \quad [2]$$

Finding such an optimal approximation  $e$  is a Nondeterministic Polynomial (1). This may be proved by demonstrating that the “exact coverage by the problem with 3 sets” (2) can be transformed into a polynomial of time in an optimal approximation problem  $e$ . Thus, an algorithm that solves the approximation problem  $e$  can solve the “exact 3-set problem coverage” which is known to be complete for the nondetermined polynomial (3).

It may be said that the optimal representation - or all the information needed to compute it - is gathered in a sequence of numbers that constitute a dynamic series for which we lack any efficient way of solving.

Another problem arises from the fact that such an optimal extension would be unstable relative to the number of  $M$  waveforms used, since the modification of  $M$ , even by only one, may lead to the complete modification of the set of waveforms chosen for representation.

These problems force us to choose sub-optimal solutions. A suboptimal extension of a function over such a redundant dictionary may be found by using the matching pursuit algorithm.

In the first step of the iterative procedure a  $g_I$  vector is chosen which gives the largest product with the signal  $f(t)$ :

$$f - \langle f, g_I \rangle g_I - R^\perp f \quad [3]$$

Then the remaining vector  $R_I$  obtained after approximating function  $f$  in direction  $g$  is similarly decomposed. The iterative procedure is repeated until one obtains as results:

$$R^n f = \langle R^n f, g_I \rangle g_I - R^{n+1} f \quad [4]$$

In this way signal  $f$  is decomposed into a sum of time-frequency atoms chosen to optimally adjust the signal residues:

$$f - \sum_{n=0}^m \langle R^n f, g_I \rangle g_I - R^{m+1} f \quad [5]$$

It has been demonstrated (1) that the procedure converges to  $f(t)$ , i.e.:

$$\lim_{m \rightarrow \infty} |R^m f| = 0 \quad [6]$$

Hence :

$$f(t) = \sum_{n=0}^m \langle R^n f, g_I \rangle g_I \quad [7]$$

and

$$|f|^2 = \sum_{n=0}^m |\langle R^n f, g_I \rangle g_I|^2 \quad [8]$$

You can view the decomposition results using the matching pursuit algorithm in the time-frequency plane by adding the Wigner distribution (4) to each of the selected atoms. The Wigner distribution of function  $f(t)$  is defined as:

$$Wf(t, \omega) = \frac{1}{2\pi} \int_{-\infty}^{\infty} f(t+\tau) f(t-\tau) e^{-i\omega\tau} d\tau \quad [9]$$

The calculation of the Wigner distribution throughout the whole decomposition as defined in equation [7] would yield:

$$Wf(t, \omega) = \sum_{n=0}^m |\langle R^n f, g_I \rangle g_I|^2 W_{g_I}(t, \omega) \quad [10]$$

$$\sum_{n=0}^{\infty} \sum_{m=0, m \neq n}^{\infty} \langle R^n f, g_I \rangle \langle R^m f, g_I \rangle W_{[g_I, g_I]}(t, \omega)$$

where the transversal Wigner distribution  $W[f, h](t, \omega)$  of functions  $f$  and  $h$  is defined by:

$$W[f, h](t, \omega) = \frac{1}{2\pi} \int_{-\infty}^{\infty} f(t-\tau) h(t+\tau) e^{-i\omega\tau} d\tau \quad [11]$$

The double sum of equation [10], which contains the Wigner cross-sectional distribution of the different atoms in extension [7] corresponds to the transversal terms generally present in the Wigner distribution. These terms need to be removed in order to get a clear picture of the energy distribution in the time-frequency representation. The removal of these terms from equation [10] is direct - we only keep the first sum. Consequently, for the visualization of the energy density in the time-frequency plane of the representation of the signal obtained by the matching pursuit filter one defines an  $Ef(t, \omega)$  variable as:

$$Ef(t, \omega) = \sum_{n=0}^m |\langle R^n f, g_I \rangle g_I|^2 W_{g_I}(t, \omega) \quad [12]$$

The Wigner distribution of a  $g_I$  atom

preserves its energy in the time-frequency plane:

$$\iint_{-\infty}^{\infty} Wg(t, \omega) dt d\omega = |g_I|^2 - 1 \quad [13]$$

By combining it with the energy conservation of the matching pursuit extension [equation (8)] and equation (11) one obtains:

$$\iint_{-\infty}^{\infty} Ef(t, \omega) dt d\omega = |f|^2 \quad [14]$$

This justifies the interpretation of variable  $Ef(t, \omega)$  as the energy density of signal  $f(t)$  in the time-frequency plane. All references in this article to “Wigner Maps” are based on formula [12] - except for the fact that that the sum is not infinite.

The method of highlighting the point where iterations should be stopped will be discussed in the next chapter.

### Simulations and practical observations

Figure 1 shows the components of the simulated signals for the purpose of presenting the time-frequency methods. The signal base, marked IV, is a sum of signals I, II and III, that were drawn to clearly present the determining structures.

Structure A is a sine wave modulated with Gauss's fourth power, structure C is constructed from straight lines while structures D and E are Gabor functions, i.e. Gaussian-modulated sinusoids. They have different modulation frequencies and widths and are centered at the same point in time. Structure B is derived from the delta Dirac function (single point discontinuity).

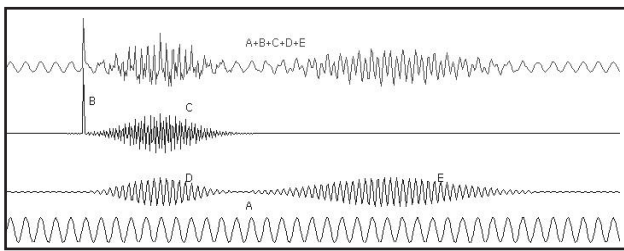


Figure 1. Components of simulated signals.

### 3.1 The matching pursuit algorithm with the dictionary of real Gabor functions

EEG records that need to be processed numerically are real and discrete series in time. In order to analyze these signals a dictionary of real time frequency atoms should be compiled, generated in accordance to equation [1]:

$$g_{(j, \phi)}(n) = K_{(j, \phi)} g_I(n-p) \cos(2\pi \frac{k}{N} n - \phi) \quad [15]$$

Index  $g = (j, k, p)$  is a discrete analogue of  $I = (x, s, u)$  in equation [1]. Assuming that the signal has  $N=2L$  samples, where  $L$  is an integer, then  $0 \leq j \leq L, 0 \leq p < N$  and  $0 \leq k < N$ .

Parameters  $p$  and  $k$  are sampled with a  $2l$  interval. Such a limited choice of parameters, similar to the dual sampling of the time-frequency space in multi-resolution damped waves is a result of the compromise between representation precision and calculations complexity.

Figure 2 shows the result of sampling the in-octave frequency domain in such a dictionary. Mention should be made that longer lasting time atoms (upper octave) have finer sampling in the frequency domain.

Parameter  $f$ , which in equation [1] was hidden as the phase of a complex number, now appears explicitly. The value of  $K_{(g, j)}$  is such that  $\frac{1}{2} g_{(g, j)}^{1/2} = 1$ . By integrating this formula [with continuous approximation] we obtain:

$$K_{(j, \phi)} = \frac{2^{1/l}}{\sqrt{2^l e^{2k/N} \cos(\frac{4\pi k p}{N} 2\phi)}} \quad [16]$$

The size of this dictionary (and the decomposition resolution) can be increased by oversampling with  $2l (l > 0)$  the time and frequency parameters  $p$  and  $k$ . The resulting dictionary has  $O(22lN \log 2N)$  waveforms, so the complexity of the calculations as well as the over-sampling increases  $2l$  times. Also, the time and frequency resolutions increase with the same factor.

$$\Delta t = 2^{-1} \frac{2^l}{f_m} \quad [17]$$

$$\Delta f = 2^{-1} \frac{f_m}{2^l} \quad [18]$$

where  $f_m$  is the sampling frequency of the analyzed signal  $f_m$ .

Here, resolution is understood as the distance between the atoms centers that are time and frequency dictionary neighbours. It depends on octave  $j$  which corresponds to the “width” of an atom in time and frequency.

The time deviation of the dictionary atoms defines our ability to measure the width in time of the signal structures represented by these atoms. It is possible to define the “width” of a time-frequency atom as half the width of the window function  $g(n)$ :

$$T_{1/2} = 2 \frac{2^l}{f_m} \sqrt{\frac{\ln 2}{\pi}} \quad [19]$$

It changes with each octave  $j$  with a factor of 2, regardless the oversampling described above.

Figure 3 shows the graphical representation of the Wigner function obtained from the decomposition based on the matching pursuit detection of simulated signal IV in Figure 1 shown at the bottom of the figure. One may notice a perfect representation of the sinusoid, of the delta Dirac function and of the two Gabor functions [B, E, C, D] that represent the waveform present in the dictionary. Adding noise does not significantly change the resolution.

### **3.2 Amplitude of a discrete Gabor function**

Variable  $\langle R^n f, g_{f_m} \rangle$  [equation [4]] algorithmically calculated for each of the selected atoms is called a module. It is the amount from the signal energy that is accounted for by a particular waveform. However, in some cases, we need the value of structures amplitude.

The relationship between the module and the amplitude of the window function of an atom in the Gabor dictionary - equation [15] - is given by equation [16]. However, this formula gives us the amplitude of the window function. The effective peak-to-peak amplitude of the corresponding Gabor function may be smaller,

depending on the frequency, phase and its octave parameters. Figure 4 shows the example of some Gabor functions in the dictionary designed from a segment of 2048 point. The window function amplitudes were normalized to 1 kHz equation [15] for all graphically drawn waveforms.

The difference between the amplitude of the Gabor function and the amplitude of the window function introduced by discrete sampling may be seen in Figure 4.

Figure 5 shows the relative difference between the double amplitude of the window function  $g$ , in equation [16], and the effective peak-to-peak amplitude of the discrete Gabor function in the frequency space.

The calculations were performed for all octaves and atomic frequencies that would form a complete discrete Gabor dictionary for a segment with 2048 intervals, averaged for over 1099 random phases. Mention should be made that only a subset of points in this plane represents the atoms actually present in the dictionary used in the calculations - compare with Figure 2. For this dictionary, there is a faster numerical implementation through the adaptation search described by Mallat and Zhang (1,3).

### **3.3 Number of development waveforms**

Another practical aspect results from the fact that normally, one does not calculate infinite developments of the terms in equation [7]. The iterations must be stopped at a certain point. The number of development waveforms can be, for example, determined by a percentage of signal dispersion resulting from the decomposition or set at a certain value. However, it is worthwhile to take a look at the behavior of the signal residue at each iteration.

The approximation of the matching pursuit filter is nonlinear and the residues, not the signal, are decomposed at each iterative stage. Their norm converges to zero, as shown in equation [6]. However, asymptotic residual properties are the key to understanding the convergence properties of the matching pursuit filter. As shown in (1), the adaptation criterion is a chaotic map. This has been proven for a particular dictionary type (2) and has been confirmed by numerical experiments.

### 3.4 Practical implementation procedures

In the brief description of the matching pursuit algorithm in Chapter 2 it was stated that at each step of the iterative procedure a vector  $g_l$  is chosen to give the largest product with the  $R^{nf}$  residue:

$$|\langle R^{nf}, g_l \rangle| - \max_l |\langle R^{nf}, g_l \rangle| \quad [20]$$

Indeed, since the dictionary compiled for a finite discrete signal has a finite number of waveforms, this condition is met by at least one of them. However, in practice, the choice of the best waveform at each stage is based on certain procedures. A direct implementation of the above selection procedure, which is already a compromise in favor of lower computing complexity, would still require an enormous amount of computing resources. It is sufficient to consider, for example, the phase, continuous by its nature, as explicitly present in the real-time frequency atoms of the Gabor dictionary. The reasonable sampling of this parameter would produce a huge dictionary even for the relatively small dimensions of the signal space [equal to the number of intervals in the analyzed signal]. Consequently, in order to make the algorithm suitable for practical applications, certain procedures for optimizing the selection procedure are implemented. Because the method, by its very nature, provides a suboptimal solution, this is not a major disadvantage by itself if the chosen processes yield reasonable results. Nevertheless, that situation should be taken into consideration if we want to compare the results obtained through various implementations of the adaptive criterion. If the implemented optimization differs even slightly, the differences accumulate at each iteration because the development is not orthogonal.

The problem of the optimal adaptation process is currently being studied. The preliminary results suggest that a selection procedure might be obtained that would improve the desired characteristics of the signal, such as, for example, the EEG morphology as perceived in the visual analysis. We believe that this research, along with advances in mathematics

and lowering the cost of computing, will make algorithms based on the adaptive criterion an acceptable parameter for biomedical signals.

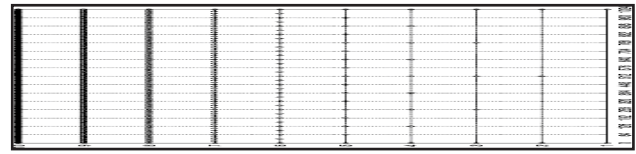


Figure 2. Sampling of frequency [on horizontal axis, 0-1024] - octave [on vertical axis, 1-10] space within the limits of the Gabor dictionary discussed in chapter 3.1.

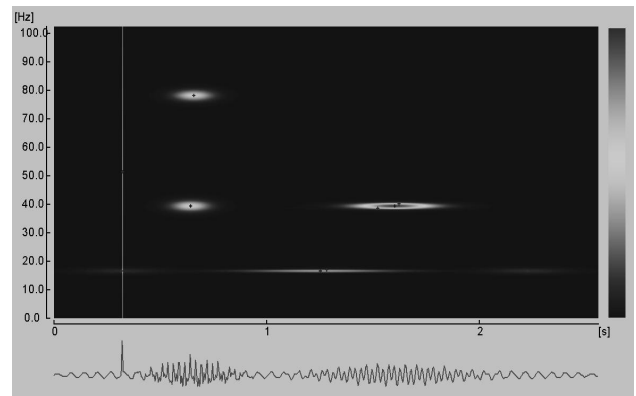


Figure 3. The Wigner representation obtained with MP for the signals shown below.

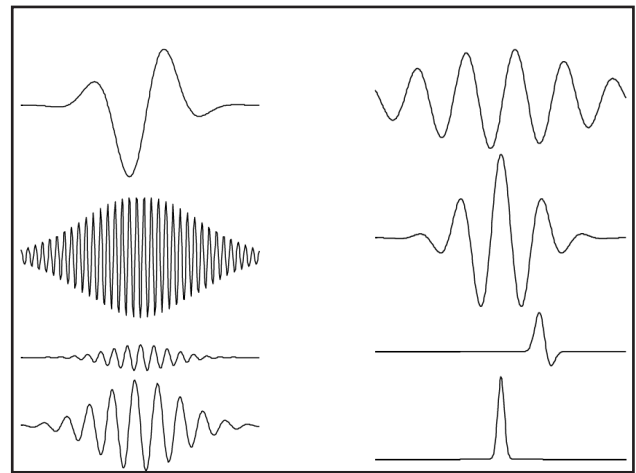


Figure 4. Examples of Gabor functions in a dictionary compiled for a segment of 2048 points. Amplitude of window function  $[K(\tau, \theta)]$  equation (15) is normalized to 1.

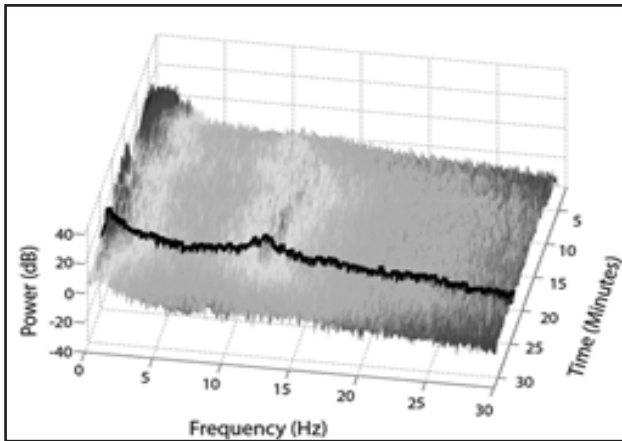


Figure 5. The relative difference between the amplitude of the window function and the instantaneous peak-to-peak amplitude of the Gabor function.

## Results and discussions

### 4.1 Detection of transient waves during sleep and their analysis based on the Matching pursuit parameterization

Peaks during sleep play a major role in analyzing brain activity during sleep.

Spontaneous rhythmic activity impulses in the 12 @ 14 Hz band, against the EEG background of a subject in the light sleeping phase were first observed in 1935 by Loomis and others, which were called “peaks” ever since.

Later, the terms sigma or sigma activity were recommended by the International Federation for Electroencephalography and Clinical Neurophysiology [IFSECN] in 1961, but their use was discouraged by IFSECN in 1974. In the “Glossary of Terms Commonly Used in Clinical Electroencephalograms” [IFSECN 1974] peaks are defined as “a group of rhythmic waves characterized by progressive growth amplitude and then gradual decrease”

The definition given in (5) states that “the presence of the peak during sleep should not be defined unless it has a duration of at least 0.5s, that is, being able to count 6 or 7 distinct waves in a half-second period. (...) The term should only be used to describe activity between 12 and 14 cycles/second”. In (6) we also find that “the peak waves are monomorphic, dysphasic and

symmetrical to the baseline. Frequency is stable in band 12 @ 14 Hz. The entire peak is variable, between 1 and 6 seconds.”

Jankel and Niedermayer (1985) also discuss the controversial appearance of peaks with a frequency around 10Hz.

Peaks during sleep show variations depending on the morphology, frequency and spatial distribution of the wave, as well as the sleeping phase. The peak map varies with age and with some disorders of the central nervous system (7). Their precise description is important in the study of insomnia, depression, aging, drug effects.

Finally, a sharper terminological clarification is given by (8): “The peak of sleep of an electroencephalograph [recorded in patients or diseased subjects] should be carefully distinguished from the peaks discussed by neurophysiologists. These are peaks recorded in experiments with animals fed on barbiturates and they served as a model for understanding the genesis of physiological EEG rhythms, such as the alpha rhythm.”

### 4.2 Choice of peaks in time-frequency atoms

The results described were obtained from two-night recordings, on sick volunteers, usually 7 hours of recorded EEG. There have been carried out numerical and visual analyses of the reference signals provided by Fz and Cz electrodes.

Segments of 20s in length [2048 points] were decomposed by using the matching pursuit algorithms (adaptive criterion) with 100 iterations per segment. Although in most cases the algorithm found coherent structures [Chapter 2], beyond this stage there were very small amplitude atoms that were far from the detection threshold.

The basic form of the waveforms in the Gabor dictionary [paragraph 3.2] is a good match for the form described in the definition of sleep time peaks [at the beginning of chapter 4]. Therefore, each peak should be represented by a time-frequency atom in this dictionary. However, in (7) we can find this warning:

“It seems clear that the term” peak “implies a bell-shaped middle surrounded by a fall to the right and left. This peak form, however, is the

exception rather than the rule. An alpha wave train resembles more the crescendo-decrescendo form of the peak. Thus, the term “peak” is wrong if sleep peaks are involved. However, it is such a “nice” and frequently used term that no terminological change can be made. “

However, as we have already said, the Gabor dictionary was chosen due to the optimal time-frequency localization of Gabor’s functions and its application is not limited to peak type structures.

The main task is to choose structures corresponding to sleep peaks from the waveforms appropriate for the analyzed segment. Such a procedure will be operational within the parameters of the appropriate atoms: time, frequency, octave, mode and phase [equation [15]].

### 4.3 Relevant parameters

Frequency. In (7) the peak frequency range was defined as covering the 12 and 14 Hz interval. In the latest works, this range has been extended by 1 Hz up and down (11 @ 15 Hz). In (8) the authors explicitly stated that “There is no doubt (...) that the range 12 @ 14 Hz is too narrow.” In this paper, the frequency range for a structure to be considered a sleep peak was set at 11 @ 15 Hz.

An octave corresponds to the wavelength of the waveform [equation [19]]. For experimental conditions [sampling frequency = 102.4 Hz, length of analyzed period N = 2048 points] the following values are obtained for half of the period of one atom T1/2] in octave j [equation [19]]:

Table 1. An octave corresponds to the wavelength of the waveform

Octave j	5	6	7	8	9
Semiperiod T1/2[s]	0,29	0,59	1,17	2,35	4,7

Octaves 6 to 8 have been chosen. The numerical values of the time and frequency resolutions [equations [18] and [19]] for these octaves are given in the table below:

Table 2. Time and frequency resolution for octaves 6 and 8

Octave j	6	7	8
Time resolution ΔT [s]	0,08	0,16	0,31
Frequency resolution Δf [Hz]	0,2	0,1	0,05

Naturally, current time is immaterial as far as classification is concerned, although it is an important parameter for evaluating results.

Finally, the main challenge is the problem of choosing amplitude parameter limits for atoms likely to be considered sleep peaks. In the definitions of sleeping peaks [chapter 4] no assumptions about amplitude were made, which naturally means that each “visible” structure that meets the criterion of time and frequency scattering should be considered a peak. This translates the problem to a lower amplitude area (or rather to the area with a lower local signal/noise ratio), which discriminates the structure against the background, with no upper limits (9).

The notion of “visibility” in the terms of the matching pursuit filter method means that the structure has been detected - that is, the optimal waveforms were determined in the iterative procedure before applying the algorithm “stop criterion” [chapter 3]. The amplitude has been left as a free parameter for the investigation of the visual and automated detection mode.

Amplitude corresponds to the parameter module that describes the dictionary’s atoms. The relationship between the module and the amplitude of the window function of an atom in the Gabor dictionary - equation [15] - is given by equation [16]. However, this formula only gives us the amplitude of the window function.

The effective peak-to-peak amplitude of the corresponding Gabor function may depend very little on the frequency and phase parameters, as shown in paragraph 3.2.

Formula [16] may be simplified for atoms that can be considered sleep peaks. They are in the octaves 6 to 8, with the frequency between 11 and 15 Hz, that corresponds to parameter k = 220 @ 300. In this case:

$$e^{-\frac{2\theta 2^{xy} k^x}{N^x}} < 1 \quad (21)$$

which gives us an approximate formula for

the window function amplitude:

$$K(\gamma, \phi) = \frac{2^{\frac{1}{\gamma}}}{\sqrt{2^l e^{\frac{2k}{N}} \cos\left(\frac{4\pi k p}{N} 2\phi\right)}} = 2^{\frac{-2^{\tau}}{\gamma}} \quad (22)$$

$$U(j \text{ module } s) = 2 - \text{module } \tau \frac{2^{\frac{-2_l \gamma}{\tau}}}{U_0} \quad [\mu V] \quad (23)$$

However, the notion of peak amplitude during sleep deduced from a visual analysis is given rather by the actual difference between the maximum and minimum values observed (measured) than by the amplitude of the envelope [10]. Furthermore, in our case, the visual analysis was performed on digitized data, as observed on the computer monitor. Due to these conditions, a correction factor was added to formula [23] in order to calculate the peak-to-peak effective amplitude instead of the window function amplitude in order to make it possible to calculate the structure amplitudes.

The automatic detection is illustrated in figures 6, 7, 8.

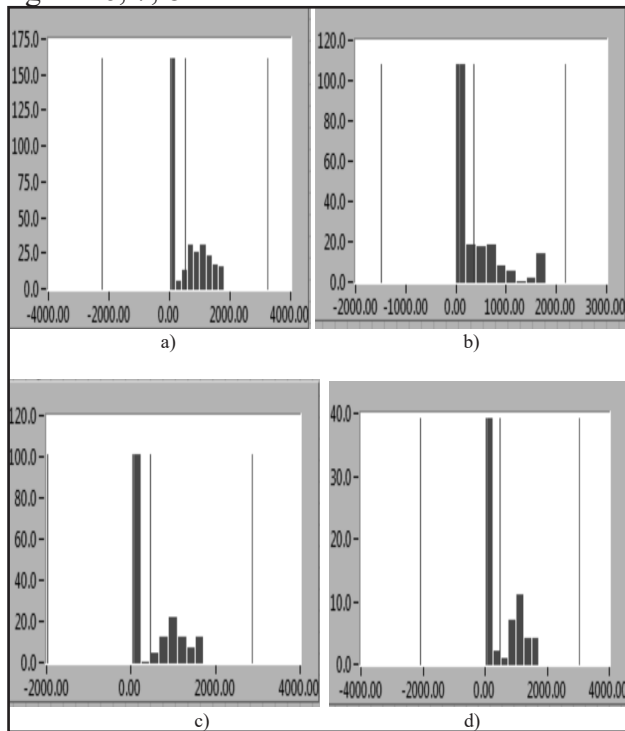


Figure 6. Automatic detection using histogram. a) TP / (TP + FP) vs. threshold amplitude b) in amplitude ranges c) and d) - detection histograms TP and FP vs. amplitude (TP - true positive, FP - false negative).

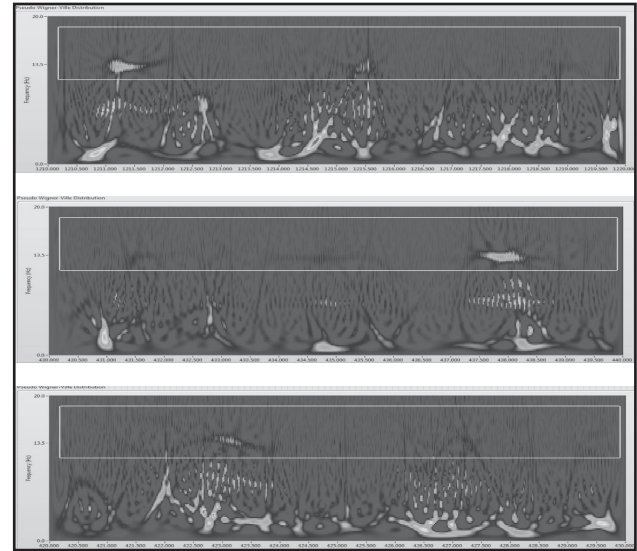


Figure 7. The same time-frequency energy (sleep spindles wave) distribution as in the previous figure, frequency increases to clearly show peaks in 12 @ 15 Hz range.

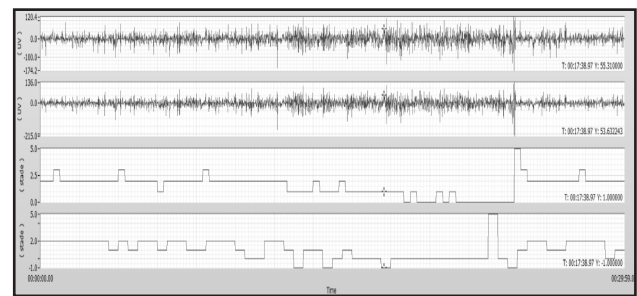


Figure 8. The peak amplitudes over time, above the hypnograms, for 21 EEG channels. The sleeping peaks detected in representations marked as sleep phase 2 activity when the transient waves appear.

The sleep spindle morphology measures from AD patient is illustrated in Figure 9.

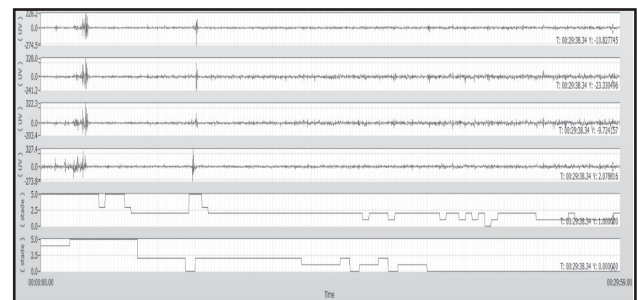


Figure 9. A typical lower sleep spindle density in an AD patient.

Finally, the methodology presented in this paper has been validated for an application with a certain degree of difficulty, namely, the detection of the K-complex and sleep spindle in the sleep

electroencephalogram (11,12).

It results from this paper that the proposed solution is among the performance solutions described in literature (12).

In addition, these results may be improved by correlating information from multiple electroencephalogram records.

## **CONCLUSION**

---

The adaptation of the representation may be improved by extending the function dictionary used to explain the signal change. The redundancy introduced in this way requires a method of choosing a subset of waveforms in the dictionary for the description of the signal.

The selection criterion can be, for example, based on minimizing the representation error for a given number of waveforms. The solution to this problem is polynomially difficult to determine, and such an optimal expansion is not stable as compared to the number of allowed waveforms. Both these problems are absent in the matching pursuit method which provides the sub-optimal solution for the problem of signal expansion as compared to a redundant dictionary.

The matching pursuit is an algorithm that iteratively adapts waveforms from a redundant dictionary to local signal structures. The Gabor Function Dictionary describes the structures present in the signal in terms of frequency, production time, time range, amplitude and phase with a resolution that can be adjusted up to their theoretical limits. Dictionaries compiled from arbitrary waveforms, not necessarily analytical functions, can be designed to improve the detection of structures with a particular morphology. However, the practical application of the matching pursuit algorithm, even for dictionaries compiled from analytical functions, requires the optimization of calculations in order to increase computing speed. This must be taken into account when comparing the results obtained with other implementations, even if the same dictionary was used.

However, it may be stated that the algorithm based on the matching pursuit algorithms makes the most complete and accurate description of the time-frequency structures of all available methods (11). This approximation offers new

possibilities for tracking EEG transitions (transient wave). The decomposition of the matching pursuit algorithm in time series can also complete a full EEG parameterization, improving the possibilities offered by previously applied methods (12).

## **Aknowledgements**

---

All authors contributed equally to this paper.

## **References**

---

1. Mallat S, Zhang Z. Matching pursuit with time-frequency dictionaries. Courant Institute of Mathematical Sciences New York United States; 1993 Jun 1.
2. Durka PJ, Ircha D, Blinowska KJ. Stochastic time-frequency dictionaries for matching pursuit. *IEEE Transactions on Signal Processing*. 2001;49(3):507-10.
3. Mallat S. Zero-crossings of a wavelet transform. *IEEE Transactions on Information theory*. 1991 Jul;37(4):1019-33.
4. Cunningham GS, Williams WJ. Fast computation of the Wigner distribution for finite-length signals. In *Acoustics, Speech, and Signal Processing, 1992. ICASSP-92., 1992 IEEE International Conference on 1992 Mar 23 (Vol. 5, pp. 177-180)*. IEEE..
5. Colrain I. M., (2005). The K-complex : A 7-decade history. *Sleep Med*, 28, pp. 255-273. [CrossRef] [PubMed]
6. Bliwise DL. Sleep disorders in Alzheimer's disease and other dementias. *Clinical cornerstone*. 2004 Jan 1;6(1):S16-28.
7. Bastuji H, García-Larrea L. Evoked potentials as a tool for the investigation of human sleep. *Sleep medicine reviews*. 1999 Mar 1;3(1):23-45.
8. Ehrhart J, Ehrhart M, Muzet A, Schieber JP, Naitoh P. K-complexes and sleep spindles before transient activation during sleep. *Sleep*. 1981 Sep 1;4(4):400-7.
9. Bastiaans MJ. Gabor's expansion of a signal into Gaussian elementary signals. *Proceedings of the IEEE*. 1980 Apr;68(4):538-9.
10. Baraniuk RG, Jones DL. Signal-dependent time-frequency analysis using a radially

Gaussian kernel. Signal processing. 1993  
Jun 1;32(3):263-84.

11. Dumitrescu C., Costea I., Badescu I., Banica C. Methodology for detection of Impose Structure. Applications of the Time-Frequency plan. Book First Edition. Bucharest, Romania: Politehnica Press; 2016.
12. Dumitrescu C., Contribution to the Processing of Biomedical Signal with TMS320C6211. Analysis of EEG signal by Pattern Recognition methods using Time-Frequency texture descriptors. PhD Thesis. A thesis submitted to the University Politehnica of Bucharest for the degree of Doctor of Philosophy. Copyright by Catalin Dumitrescu 2004.